https://doi.org/10.48048/tis.2024.7579

Gold Nanobipyramids as Plasmonic Sensor for Insecticide Detection in Lettuce

Iwantono Iwantono[1,*], Arif Darma Saputra[1], Puji Nurrahmawati[2], Mayta Novaliza Isda[3], Suratun Nafisah[4], Romi Fadli Syahputra[5] and Marlia Morsin[6]

[1]Department of Physics, Faculty of Mathematics and Natural Science, Universitas Riau, Riau, Indonesia
[2]Department of Biology, Faculty of Mathematics and Science, Universitas Riau, Riau, Indonesia
[3]Department of Electrical Engineering, Faculty of Engineering, Universitas Negeri Padang, West Sumatra, Indonesia
[4]Department of Electrical Engineering, Institute Technology of Sumatera (ITERA) Way Hui, Lampung Selatan, Indonesia
[5]Department of Physics, Universitas Muhammadiyah Riau, Riau, Indonesia
[6]Microelectronic and Nanotechnology - Shamsuddin Research Centre (MiNT-SRC), Institute of Integrated Engineering, Universiti Tun Hussein Onn Malaysia, Johor, Malaysia

([*]Corresponding author's e-mail: iwantono@lecturer.unri.ac.id)

Received: 7 October 2023, Revised: 13 December 2023, Accepted: 20 December 2023, Published: 20 May 2024

Abstract

The application of malathion, an insecticide derived from organophosphates, raises substantial apprehensions over human health in the context of pest management in agricultural produce. The presence of a lack of specialized knowledge and the intricate nature of traditional diagnostic methods have further intensified these symptoms, resulting in significant and persistent damage to the human body. The present study aims to synthesis a gold-nanobipyramids (AuNBPs) for identifying malathion and other organophosphate pollutants, even at exceedingly low levels of detection. The AuNBPs is synthesis by the utilization of the seed-mediated growth (SMG) method. The UV-Vis spectroscopy analysis has identified 2 unique absorption peaks, specifically transverse surface plasmon resonance (t-SPR) occurring between 550 and 600 nm, and longitudinal surface plasmon resonance (l-SPR) occurring within the wavelength range of 750 to 850 nm. Additional analysis of AuNBPs reveals its capacity for notable and distinctive optical resonance, particularly in the visible and near-infrared regions of the electromagnetic spectrum. This characteristic renders AuNBPs very appropriate for the development of localized surface plasmon resonance (LSPR) sensors. The sensitivity experiments conducted on the LSPR sensor based on AuNBPs have shown compelling evidence of its capability to detect malathion and other pollutants in the AuNBPs growth solution across different concentrations. These findings highlight the sensor's potential for efficient residue detection of malathion. This discovery underscores the significant importance of its function in safeguarding food safety and reducing the potential hazards linked to the utilization of malathion and other insecticides based on organophosphates in agricultural practices.

Keywords: Agriculture, AuNBPs, Insecticide, LSPR, Malathion, Nanomaterial, Sensor

Introduction

Pesticides serve to increase crop production from weeds, insects, and fungi. The utilization of pesticides in agricultural practices is a prevalent global phenomenon that serves multiple objectives, such as safeguarding crops from the detrimental effects of pests, diseases, and weeds [1,2]. Pesticides refer to chemical or biological agents that are intentionally formulated to control or eradicate factors that pose risks to agricultural productivity [3]. Eradicating or preventing animals that can cause disease in humans or animals that need to be protected by use on plants, soil or water [1,4]. Pesticides encompass 4 distinct categories, namely insecticides, herbicides, rodenticides, and fungicides. The insecticides now experiencing a rise in usage within the market include organophosphates, pyrethroids and carbamates [5].

Malathion is commonly employed in the cultivation of fruit plants, vegetables, herbaceous ornamentals, as well as trees and shrubs [6]. Malathion is employed in the agricultural sector for the purpose of pest control in plants [7]. Malathion is classified as an organophosphate pesticide, falling under class 1 [8,9]. Malathion is employed due to its comparatively reduced toxicity in comparison to other forms of

organophosphate compounds [10]. Malathion has been found to have hepatotoxic, nephrotoxic, gonadotoxic, pneumotoxic, pancreatic toxic, and hematotoxic effects [2]. Nevertheless, the central nervous system (CNS) has been documented as the primary site of toxic effects [10]. According to the findings of the study, a notable 88 % of participants reported feeling acute poisoning. This occurrence was found to have a strong correlation with the duration of exposure to pesticides, specifically those classified as belonging to classes I and II, which accounted for 50 % of the pesticides used [11].

In recent years, nanobipyramids have been successfully synthesized to detect chlorpyrifos contamination based on LSPR sensors. The results attracted researchers to test the sensor's ability to detect the presence of other pesticides such as Malathion. The utilization of gold nanopyramids (AuNBPs) as detectors for organic substances has been demonstrated through their surface plasmon resonance (SPR) feature [12,13]. The quantities of substances, such as Aflatoxin B1, have a linear relationship with the intensity of the optical spectrum [13]. The present study aimed to fabricate localized surface plasmon resonance (LSPR) sensors utilizing gold nanopyramids (AuNBPs) for the purpose of detecting malathion in lettuce plants, even at low concentrations. The analysis of sensor sensitivity encompasses both transversal surface plasmon resonance (t-SPR) and longitudinal surface plasmon resonance (l-SPR).

Materials and methods

Materials and reagents

The materials utilized for the synthesis of AuNBPs as a detection material include cetyltrimethylammonium bromide (CTAB) obtained from Sigma Aldrich, gold (III) chloride trihydrate ($HAuCl_4.H_2O$) also obtained from Sigma Aldrich, Chloroplatinic acid hydrate ($H_2PtCl_4.H_2O$) from Sigma Aldrich, sodium borohydride ($NaBH_4$), silver nitrate ($AgNO_3$) from Honeywell, hydrochloric acid (HCl) from Sigma Aldrich, L-ascorbic acid ($C_6H_8O_6$) from Sigma Aldrich and Malathion produced by Hextar Global Bhd in Malaysia.

Synthesis

The production of AuNBPs is achieved through a 2-stage process, consisting of seeding and growth. The synthesis technique employed in this study is commonly referred to as seed mediated growth (SMG) [14,15]. The seeding procedure involved the preparation of a 10 mL solution combination containing 0.01 M $HAuCl_4$, 0.1 M CTAB, 0.01 M H_2PtCl_4 and 0.01 M $NaBH_4$. Following the preparation, the homogenous solution was allowed to age for a period of 2 h.

Second step is growth process. The growth process commences by homogeneously combining a solution of 0.1 M CTAB with a solution of 0.01 M $HAuCl_4$, as well as a solution of 0.01 M H_2PtCl_4 with a solution of 0.01 M $AgNO_3$. In addition, the experimental procedure involved the addition of a 1 M hydrochloric acid solution, a 0.01 M silver nitrate solution and a 0.1 M ascorbic acid solution. The solution functions as a reducing agent in the growth solution. Subsequently, the previously prepared seeding solution with a concentration of 0.05 M is introduced, and the efficacy of AuNBPs is assessed following a 2-hour incubation period at a temperature of 25 °C. The growth solution was applied over a substrate of fluorine tin oxide (FTO) in order to examine the morphology using field emission scanning electron microscopy (FESEM). The instrument employed in this study is the JEOL JSM-7600 F Schottky FESEM.

Target analyte preparation

The lettuce plants were collected when reaching a maturity of 10 days, followed by the applying 2.5 mL of malathion dissolved in 500 mL of distilled water as an insecticide. The lettuce plants were subjected to the application of Malathion. Subsequently, the lettuce underwent a series of rinses. This rinsing cycle is done to pick up insecticide residue on the same lattuce. The utilized modifications encompassed rinses numbered 1, 2, 3 and 4. The concentrations derived from the rinsing process were found to be 16 mg/L for a single rinse, 9 mg/L for 2nd rinses, 7 mg/L for 3rd rinses and 3 mg/L for last rinses. The residual malathion obtained from the rinsed lettuce samples was referred to as the target analyte.

Sensor set up

The sensor system designed for the detection of malathion consists of several components. These include a sensor chamber, an AvaLight-HAL-S-Mini halogen light source (Avantes), which emits light within the wavelength range of 260 - 2,500 nm to stimulate the LSPR properties on the surface of AuNBPs. The system also incorporates a SE-P400-2-UV-SWIR duplex optical fiber provided by Ocean Optics, featuring a core diameter of 400 µm. This fiber is responsible for transmitting the light emitted by the light source to the AuNBPs sample and subsequently forwarding the reflected light to the Flame-S-XR1

spectrometer, also manufactured by Ocean Optics. The spectrum study was conducted using the Computer and OceanView 1.6.5 software developed by Ocean Optic, a company based in the United States. The assembly of the sensor set up was performed manually.

The testing

The AuNBPs were synthesized and utilized as sensing agents for the purpose of detecting the presence of specific target analytes. The target analyte with a volume of 0.5 mL was thoroughly mixed with AuNBPs until a uniform mixture was achieved. The solution has been determined for the purpose of conducting sensitivity, stability and repeatability testing.

Results and discussion

Optical and structural properties

The AuNBP, which comprises 2 pyramids that combine to produce a unified particle, was subjected to analysis using a range of characterisation techniques. **Figure 1** presents a graphical depiction of the light intensity distribution, showcasing the physical parameters derived from variations in the samples' synthesis time. These time intervals include 30 min (0.5 h), 60 min (1 h), 120 min (2 h) and 240 min (3 h). This variation functions as a parameter for the optimization of AuNBP growth.

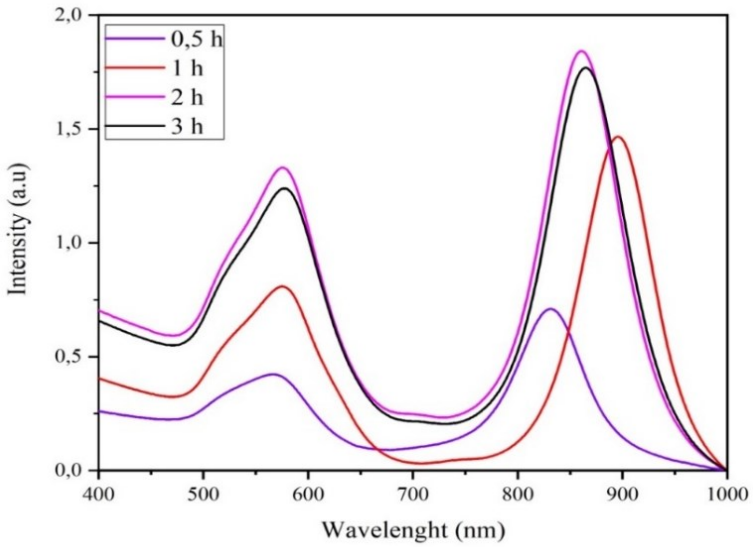

Figure 1 UV-Vis spectra of AuNBPs.

The UV-Vis analysis provides a clear depiction of distinct peaks that correlate to the surface resonance of AuNBP. These peaks encompass both the l-SPR and t-SPR peaks. The graph illustrates that the l-SPR peak is detected within the wavelength range of 700 - 900 nm. The t-SPR absorption peak is observed within the wavelength range of 500 - 600 nm. The shoulder observed in the t-SPR peak, which manifests at a wavelength of approximately 520 nm, is associated with the SPR induced by the nanomaterials. The monitoring of the stability of the synthesized AuNBP material is being conducted in order to ascertain that the samples demonstrate satisfactory durability throughout the testing procedure.

AuNBPs have been utilized in prior studies as LSPR sensors for the detection of glyphosate [12,16], as well as for colorimetric [17] and IgG sensing applications [18]. The findings of this investigation align with the previous work which also observed the presence of pyramidal shapes [19]. It is evident that AuNBPs do not only manifest in one particular form, as there are alternative forms such pyramids. The AuNBPs utilized in this research exhibit a mean length of 81.32 ± 16.52 nm, a mean diameter of 36.62 ± 4.55 nm, and a mean surface density of 54.43 ± 1.53 %. According to the histogram data presented in **Figure 1(b)**, the majority of the produced AuNBPs have a diameter size ranging from 35 to 40 nm. The structural properties of AuNBPs are presented in **Table 1**.

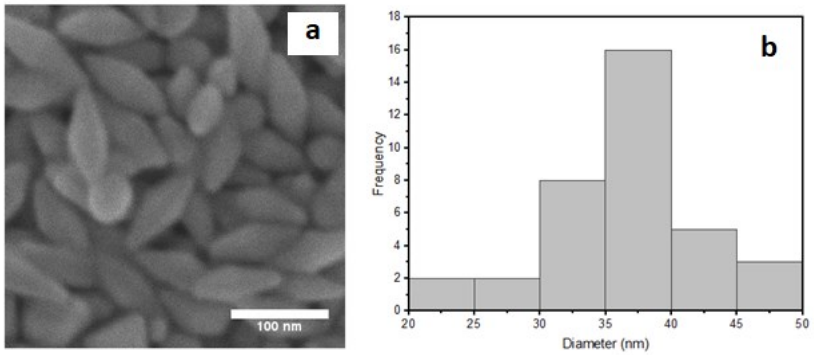

Figure 2 (a) FESEM images of AuNBPs and (b) its histogram of diameter.

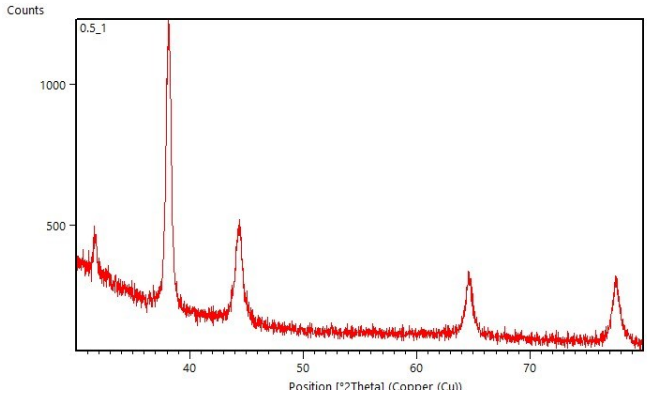

Figure 3 XRD pattern of AuNBP.

Figure 3 displays a XRD pattern characterized by the presence of 4 distinct peaks located at certain angles 2θ: 38.14, 44.30, 64.64 and 77.48 °. The analysis reveals a distinct diffraction pattern with high intensity and a narrow full width at half maximum (FWHM) value. The results align with the established Inorganic Crystal Structure Database (ICSD) reference number 04-0783 [14]. These observations indicate the material's remarkable crystalline quality. It is worth mentioning that AuNBP has a crystal structure characterized by distinct orientations of crystal planes.

The sensitivity

The AuNBPs LSPR sensor demonstrates success in the sensitivity test, as indicated by the presence of 2 absorption peaks in the wavelength spectrum, specifically the t-SPR and l-SPR peaks [20]. In this study, the analysis of **Figure 1** reveals the presence of 2 distinct absorption peaks. The initial peak occurs within the wavelength range of 450 - 550 nm, commonly referred to as the t-SPR mode. The 2nd peak corresponds to a wavelength range of 600 - 800 nm, commonly referred to as the l-SPR mode. The absorption peak range exhibited by AuNBPs when combined with the target analyte bears resemblance to the findings documented by Suratun in their investigation on glyphosate detection [12]. The absorption outcomes observed in this study are consistent with the absorption properties of AuNBPs in the absence of being combined with the reference target analyte.

Figure 4 illustrates the observed shift in absorption at the peaks corresponding to the t-SPR and l-SPR at the greatest peak. The strength of both peaks has a negative correlation with the number of malathion rinses applied to lettuce. This phenomenon can be attributed to the increased number of rinses conducted, which leads to a reduction in the concentration of malathion. The intensity in t-SPR exhibited a reduction from 1.32×10^4 to 1.15×10^4 a.u., where as the intensity in l-SPR decreased from 4.5×10^4 to 4.07×10^4 a.u.

Further analysis reveals a positive correlation between the concentration of malathion and the strength of the LSPR response. This phenomenon arises as a result of an elevation in the refractive index. The influence on the response of this sensor is additionally affected by alterations in the refractive index [19,21] and dielectric constant of the surrounding medium [12]. Variations in the refractive index of malathion can induce alterations in the dielectric constant. The alterations in refractive index and dielectric properties have

a discernible influence on the interaction between nanoparticles and light. This interaction is characterized by the absorption and scattering of photons, which aligns with the relevant LSPR process. The outcome of this phenomenon is the formation of a highly concentrated electromagnetic field in the immediate vicinity. This field is produced through the LSPR effect, causing the nanoparticles to function as transducers with a heightened responsiveness to alterations in the local refractive index [22]. Simply put, AuNBP's respon to malathion shown by the increase in sensitivity at each different concentration demonstrate that the LSPR AuNBPs sensor maintains a satisfactory level of sensitivity even when subjected to 4 rounds of lettuce flushing.

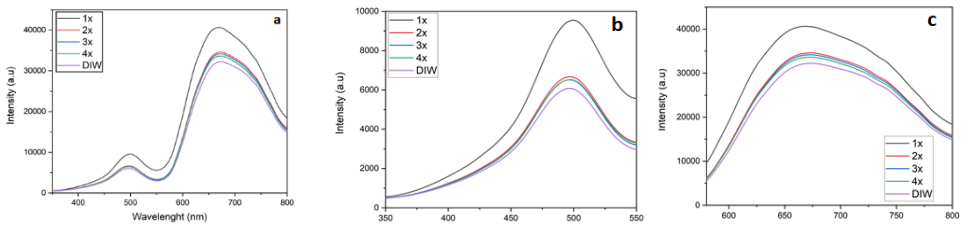

Figure 4 (a) Sensitivity of AuNBP for different malathion concentration. Sensitivity of (b) t-SPR, and (c) l-SPR.

The stability

The stability assessment of the LSPR sensor was performed for a duration of 600 s. The stability of the LSPR sensor was assessed by quantifying the peak spectrum intensity in both the malathion solution (MAL) and deionized water (DIW). The outcomes of the stability assessment are visually depicted in **Figure 5**.

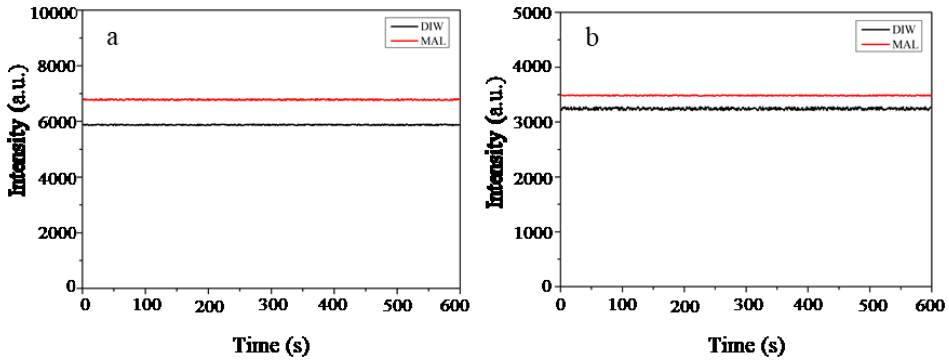

Figure 5 Stability test over 600 s measurements for (a) t-SPR and (b) l-SPR modes.

The intensity of AuNBPs was measured in 2 distinct solutions, namely DIW and MAL solutions, within the framework of the l-SPR and t-SPR peak. The measured intensity values for DIW and MAL were 3.21×10^5 and 3.48×10^5 a.u, while the t-SPR is 5.84×10^4 and 6.76×10^4 a.u, respectively. It is noteworthy to notice that the intensity of MAL, namely at both the l-SPR and t-SPR peaks, displayed a greater magnitude when compared to DIW. This demonstrates the efficacy of AuNBPs in effectively mitigating the presence of malathion residues. No extended reach significant difference was seen in the intensity of AuNBPs in relation to MAL throughout the specified time period. The stability tests that were done confirm the considerable potential of the plasmonic sensor utilizing AuNBPs for a range of detecting applications.

The repeatability

In order to ascertain the reproducibility of the plasmonic sensor in its ability to detect malathion, the AuNBPs was subjected to many tests using DIW and MAL concentration of 16 mg/L. Each test lasted for a duration of 60 s. The experimentation was carried out at a wavelength of 498.661 nm to see the t-SPR peak and 667.051 nm to observe the l-SPR peak. Each cycle was repeated a total of 5 times for both peaks. The experimental results and average intensities for each period are depicted in **Figure 6(a)**. The repeatability of the reaction, as depicted in **Figure 6**, is found to be excellent over 5 testing cycles. This phenomenon is apparent when the MAL intensity consistently reverts back to its initial intensity at the onset of every cycle.

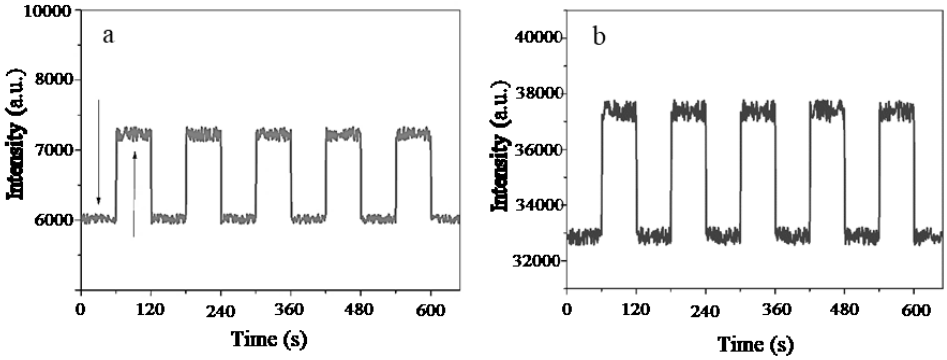

Figure 5 Repeatability of (a) t-SPR and (b) l-SPR modes.

Conclusions

The synthesis of AuNBPs was successfully achieved using the SMG technique. Structural property of AuNBPs, which exhibited a length of 79.14 ± 0.56 nm and a diameter of 36.72 ± 0.55 nm. Furthermore, the UV-Vis analysis revealed absorbance measurements at specific wavelengths of 550 nm corresponding to t-SPR mode and 750 nm corresponding to l-SPR mode. The XRD spectra exhibited distinct 4 diffraction peaks at specific 2θ angles, which can be attributed to the crystal plane orientations of (111), (200), (220) and (311). The plasmonic sensor demonstrated heightened sensitivity to malathion, as evidenced by a rise in values corresponding to the concentration of the residual solution. The obtained results demonstrate that the intensity of AuNBPs in the presence of malathion was significantly increased compared to that in deionized water. This finding suggests that AuNBPs exhibits a strong and effective reaction to the presence of malathion residue. Moreover, the intensity of AuNBPs in relation to malathion did not demonstrate a statistically significant range, with an average value of 0.005 a.u. There is a prevailing belief that the use of AuNBPs as a detection material in plasmonic sensors has the capacity to augment sensitivity efficiency towards malathion, hence exhibiting significant prospects for future detection applications.

Acknowledgements

This work was funded by Ministry of Education, Culture, Research, and Technology of Indonesia through LPPM Universitas Riau under research scheme of "Penelitian Fundamental" (Grant No. 15474/UN19.5.1.3/AL.04/2023). Authors also thanks to Universitas Riau, Indonesia and Micro-electronics and Nanotechnology – Shamsuddin Research Center (MiNT-SRC) for the laboratory facilities.

References

[1] A Sharma, A Shukla, K Attri, M Kumar, P Kumar, A Suttee, G Singh, RP Barnwal and N Singla. Global trends in pesticides: A looming threat and viable alternatives. *Ecotoxicol. Environ. Saf.* 2020; **201**, 110812.

[2] A Sharma, V Kumar, B Shahzad, M Tanveer, GPS Sidhu, N Handa, SK Kohli, P Yadav, AS Bali, RD Parihar, OI Dar, K Singh, S Jasrotia, P Bakshi, M Ramakrishnan, S Kumar, R Bhardwaj and AK Thukral. Worldwide pesticide usage and its impacts on ecosystem. *SN Appl. Sci.* 2019; **1**, 1446.

[3] M Shokrzadeh and SSS Saravi. *Pesticides in Agricultural products: Analysis, reduction, prevention*. *In*: M Stoytcheva (Ed.). Pesticides - formulations, effects, fate. Intechopen Limited, London, 2011, p. 225-42.

[4] R Leoci and M Ruberti. Pesticides: An overview of the current health problems of their use. *J. Geosci. Environ. Protect.* 2021; **9**, 1-20.

[5] IP Andika and E Martono. Mapping of Indonesia's agricultural insecticide in 2021: Registered Products, future research opportunities, and information dissemination. *AGRIVITA J. Agr. Sci.* 2022; **44**. 377-89.

[6] A Hala and S Gaffar. Could organic pesticides be a good alternative to synthetics in controlling aphids and leafhoppers in tomato fields? *J. Plant Protect. Pathol.* 2020; **11**. 127-34.

[7] FG Taherdehi, MR Nikravesh, M Jalali, A Fazel and MG Valokola. Evaluating the protective role of ascorbic acid in malathion-induced testis tissue toxicity of male rats. *Int. J. Prev. Med.* 2019; **10**, 45.

[8] M Reza, J Fiza, F Hossen and F Ahmed. Isolation and partial characterization of organophosphate

pesticide degrading bacteria from soil sample of Noakhali, Bangladesh. *Bangladesh J. Microbiol.* 2019; **36**, 17-22.
[9] K Tamanna, B Prerna and S Vineeta. Assessment of an organophosphate pesticide particularly malathion on earthworm: A review. *Int. J. Zool. Investig.* 2022; **8**. 568-77.
[10] AM Badr. Organophosphate toxicity: Updates of malathion potential toxic effects in mammals and potential treatments. *Environ. Sci. Pollut. Res.* 2020; **27**, 26036-57.
[11] HK Jensen, F Konradsen, E Jørs, JH Petersen and A Dalsgaard. Pesticide use and self-reported symptoms of acute pesticide poisoning among aquatic farmers in phnom penh, cambodia. *J. Toxicol.* 2011; **2011**, 639814.
[12] S Nafisah, M Morsin, R Sanudin, NL Razali, ZM Zain and M Djamal. Gold nanobipyramids as LPSR sensing materials for glyphosate detection: Surface density and aspect ratio effect. *IEEE Sens. J.* 2022; **22**, 18479-85.
[13] H Bhardwaj, G Sumana and CA Marquette. Gold nanobipyramids integrated ultrasensitive optical and electrochemical biosensor for aflatoxin B1 detection. *Talanta* 2021; **222**, 121578.
[14] DW Jung, JM Kim, HJ Yun, GR Yi, JY Cho, H Jung, G Lee, WS Chae and KM Nam. Understanding metal-enhanced fluorescence and structural properties in Au@Ag core–shell nanocubes. *RSC Adv.* 2019; **9**. 29232-7.
[15] S Nafisah, Iwantono, M Morsin, Y Citra, S Melani and NL Razali. Optical properties of the amine functionalized gold nanobipyramids: Effect of functionalization times period. *Int. J. Nanoelectronics Mater.* 2020; **13**. 615-24.
[16] S Nafisah, M Morsin, NA Jumadi, N Nayan, NSM Shah, NL Razali and NZ An'Nisa. Improved sensitivity and selectivity of direct localized surface plasmon resonance sensor using gold nanobipyramids for glyphosate detection. *IEEE Sens. J.* 2020; **20**, 2378-89.
[17] Y Xue, X Ma, X Feng, S Roberts, G Zhu, Y Huang, X Fan, J Fan and X Chen. Temperature-derived purification of gold nano-bipyramids for colorimetric detection of tannic acid. *ACS Appl. Nano Mater.* 2023; **6**, 11572-80.
[18] H Zhang, Z She, H Su, K Kerman and HB Kraatz. Effects of bipyramidal gold nanoparticles and gold nanorods on the detection of immunoglobulins. *Analyst* 2016; **141**, 6080-6.
[19] S Nengsih, AA Umar, MM Salleh and M Oyama. Detection of formaldehyde in water: A shape-effect on the plasmonic sensing properties of the gold nanoparticles. *Sensors* 2012; **12**, 10309-25.
[20] S Nafisah, M Morsin, I Iwantono, R Sanudin, ZM Zain, L Satria, NL Razali and D Mardiansyah. Growth time dependency on the formation of gold nanobipyramids for efficient detection towards chlorpyrifos-based LSPR sensor. *Optik* 2023; **289**, 171270.
[21] J Jeon, S Uthaman, J Lee, H Hwang, G Kim, PJ Yoo, BD Hammock, CS Kim, YS Park and IK Park. In-direct localized surface plasmon resonance (LSPR)-based nanosensors for highly sensitive and rapid detection of cortisol. *Sensor. Actuator. B Chem.* 2018; **266**, 710-16.
[22] YA Hong and JW Ha. Enhanced refractive index sensitivity of localized surface plasmon resonance inflection points in single hollow gold nanospheres with inner cavity. *Sci. Rep.* 2022; **12**, 6983.